

Load Balancing-based Topology Adaptation for Integrated Access and Backhaul Networks

Raul Victor de O. Paiva, Fco. Italo G. Carvalho, Fco. Rafael M. Lima, Victor F. Monteiro, Diego A. Sousa, Darlan C. Moreira, Tarcisio F. Maciel and Behrooz Makki

Abstract—Integrated access and backhaul (IAB) technology is a flexible solution for network densification. IAB nodes can also be deployed in moving nodes such as buses and trains, i.e., mobile IAB (mIAB). As mIAB nodes can move around the coverage area, the connection between mIAB nodes and their parent macro base stations (BSs), IAB donor, is sometimes required to change in order to keep an acceptable backhaul link, the so called topology adaptation (TA). The change from one IAB donor to another may strongly impact the system load distribution, possibly causing unsatisfactory backhaul service due to the lack of radio resources. Based on this, TA should consider both backhaul link quality and traffic load. In this work, we propose a load balancing algorithm based on TA for IAB networks, and compare it with an approach in which TA is triggered based on reference signal received power (RSRP) only. The results show that our proposed algorithm improves the passengers worst connections throughput in uplink (UL) and, more modestly, also in downlink (DL), without impairing the pedestrian quality of service (QoS) significantly.

Index Terms—mIAB, topology adaptation, load balancing.

I. INTRODUCTION

The use of the large available bands in millimeter wave (mmWave) frequencies in fifth generation (5G) networks allows the fulfillment of quality of service (QoS) requirements for new data-hungry services. However, that part of the spectrum suffers from severe path and penetration losses [1], [2]. To overcome these drawbacks, one envisioned solution is the densification of the network with integrated access and backhaul (IAB) nodes.

In summary, an IAB node can be seen as a regular gNodeB (gNB) in which the backhaul is wireless, being served by another network node, called IAB donor. IAB nodes enable deploying new infrastructure avoiding the high costs and time consumption of traditional wired installations and overcoming possible limitations on trenching, such as in historical places [3]–[6].

In Release 18 [7], it was investigated applications and technical requirements for 5G networks that use vehicle-mounted relays (VMRs) that provide service to

onboard passengers and surrounding pedestrians. Additionally, VMRs are designed to facilitate seamless connectivity despite the mobility of the user equipments (UEs) and the VMR itself. For IAB networks, VMRs can be identified as mobile IAB (mIAB) [7].

Topology adaptation (TA), in this context, refers to the migration of an IAB node from an IAB donor to another one, which is triggered when the link between an IAB node and its current donors weakens, due to mobility and/or obstacles [8]. As mIAB nodes move, the traffic load in the system becomes more dynamic and heterogeneous. Specifically, in a given instant of time, one macro base station (BS) may serve only a few pedestrians, while other macro BSs may serve several mIAB nodes through their backhaul as well as direct pedestrians. Thus, depending on the system load distribution, not all IAB donors can provide satisfactory backhaul service to a coming mIAB node, due to the lack of available radio resources.

The authors in [9] surveyed several works on IAB and mIAB and presented a detailed performance evaluation in order to assess the gains of mIAB over conventional deployments. It was shown that the load variability among IAB donors is in general high with mIAB nodes. The authors then discussed the need of TA strategies that consider IAB donor load to avoid overloading IAB donors.

In [10], the authors proposed a method to distribute the load among fixed IAB nodes efficiently by sharing their load information and data processing capabilities. The proposed method outperformed traditional approaches based on metrics such as reference signal received power (RSRP) in terms of average throughput and number of served UEs. Motivated by the conclusions of [9], [10] and use cases involving load balancing in Release 18 [7], we investigate load balancing based TA in this paper.

In this letter, we propose a TA strategy that takes into account not only the channel strength but also the system load in a mIAB network. Results show that our proposed solution outperforms the standard TA solution, leading to improved throughput for passengers without significantly deteriorating the pedestrians' QoS.

II. MOBILE INTEGRATED ACCESS AND BACKHAUL

The IAB architecture, illustrated in Fig. 1, was designed to support multiple wireless backhaul hops in new radio (NR). Therein, the blue boxes represent the IAB nodes. These nodes can connect to each other wirelessly. The IAB donors, shown

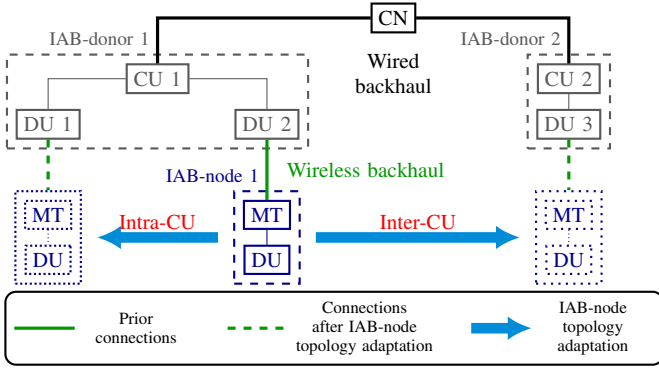


Fig. 1. Illustration of IAB NR architecture with IAB donor and nodes main components and topology adaptation [9].

as gray boxes, have a wired backhaul and provide wireless backhaul to an IAB node.

The IAB nodes can be split into distributed unit (DU) and mobile termination (MT) [11]. The MT component is responsible for managing the radio signal used to connect to a parent node that can be an IAB donor or an IAB node. The DU component serves as the NR interface for both UEs and the MT part of a child IAB node. The IAB donors, with wired backhaul to the core network (CN), have two parts: centralized unit (CU) and DU. Lower protocol layers are responsibility of the DUs, while the upper protocol layers are provided by the CUs [11]. The aforementioned split permits time-critical functionalities to be conducted in the DU near the served nodes, while others are handled with more processing power in the CU [4].

Wireless backhaul allows for the deployment of mobile cells, the mIAB nodes, that can provide uninterrupted cellular services for moving UEs [9]. The main use cases for mIAB technology consist in the service provision for both passengers onboard and pedestrians in the adjacency of the vehicle [7]. For buses, the outer antennas on top correspond to the MT, while the inner antennas correspond to the DU.

Concerning TA, an IAB node might need to switch to a different parent node after initial setup. This can happen, for example, if the connection to its current parent weakens due to movement or obstructions between them [8]. In fixed IAB scenarios, TA due to poor channel quality is less frequent, as nodes are stationary and well planned. In contrast, in mIAB scenarios, TA mainly occurs due to channel variations caused by the movement of transmitters and receivers [8].

Figure 1 shows a TA illustration for IAB node 1 in a scenario with two IAB donors (donors 1 and 2). Assuming IAB node 1 as an mIAB, we can see that it has donor 1 (through DU 2) as parent node and needs to switch to another parent node due to poor backhaul link quality. Donor 1 (through DU 1) and donor 2 are candidate parent nodes. In this case, donor 1 through DU 1 may provide a connection with the same IAB donor-CU (intra-CU), while donor 2 may provide a different IAB donor-CU (inter-CU). The inter-CU case involves handover requests [8].

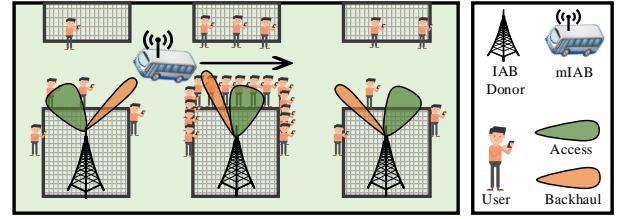


Fig. 2. Scenario of interest.

III. SYSTEM MODEL AND LOAD-AWARE TOPOLOGY ADAPTATION

In Fig. 2, the proposed study scenario is shown. It considers a single bus equipped with an mIAB, which is connected to an IAB donor and, as the time passes, gets closer to two other donors, the closest (center) one being overloaded.

Conventionally, the mIAB node performs TA to the IAB donor that provides the strongest backhaul link quality, e.g., highest RSRP, which is usually the closest one. However, in the considered scenario, the choice of the IAB donor with stronger RSRP may degrade the connection of onboard UEs, since the the closest IAB donor is overloaded. Thus, few radio resources would be left for backhaul connection.

A solution for this situation is to avoid the connection of the incoming mIAB node, i.e., TA, to the overloaded IAB donor and connecting it to another, less loaded, IAB donor instead. Therefore, to that end, the following Algorithm 1 is proposed. It aims at selecting a candidate IAB donor to which to handover the mIAB node. It takes into account not only the RSRP of a candidate IAB donor, but also its load, represented by the quantity of buffered bits at the IAB donors. Specifically, besides of having an RSRP value greater than a selected minimum value (line 4) and an RSRP not significantly smaller than the RSRP value of the current IAB donor (line 5), the candidate serving IAB donor must have a traffic load smaller than the current serving one (line 3).

The main objective of this work is to compare a standard TA algorithm [9] which considers only the RSRP value as activation criterion, hereafter called standard algorithm, against the proposed Algorithm 1.

IV. PERFORMANCE EVALUATION

This section presents a performance comparison between the standard and the proposed TA algorithms. The main simulation parameters are presented in subsection IV-A and the results are discussed in subsection IV-B.

Algorithm 1: Update Parent Base Station

Input: List of IAB donors: *donors*
Output: Updated parent IAB donor: *parent*

```

1 foreach candidate in donors do
2   if candidate is not parent then
3     if candidate.bits < parent.bits then
4       if candidate.RSRP > minRSRP then
5         if candidate.RSRP > parent.RSRP -
           minRSRPDiff then
6           parent ← candidate;

```

TABLE I
ENTITIES CHARACTERISTICS.

Parameter	IAB donor	mIAB node		UE	
		DU	MT	Ped.	Pass.
Height	25 m	2.5 m	3.5 m	1.5 m	1.8 m
Transmit power	35 dBm	24 dBm	24 dBm	24 dBm	24 dBm
Antenna tilt	12°	4°	0°	0°	0°
Antenna array	ULA 64	URA 8×8	ULA 64	Single antenna	Single antenna
Antenna element pattern	3GPP [14]	3GPP [14]	Omni	Omni	Omni
Max. antenna element gain	8 dBi	8 dBi	0 dBi	0 dBi	0 dBi
Speed	0 km/h	50 km/h	50 km/h	3 km/h	50 km/h

TABLE II
SIMULATION PARAMETERS.

Parameter	Value
Layout	Simplified Madrid grid [12], [13]
Carrier frequency	28 GHz
Subcarrier spacing	60 kHz
Number of subcarriers per RB	12
Number of RBs	22
Slot duration	0.25 ms
OFDM symbols per slot	14
Channel generation procedure	As described in [14, Fig. 7.6.4-1]
Path loss	As described in [14, Table 7.4.1-1]
Fast fading	As described in [14, Sec.7.5] and [14, Table 7.5-6]
AWGN power per subcarrier	-174 dBm
Noise figure	9 dB
Mobility model	Pedestrian and Vehicular [15]
Number of buses	1
Passengers + pedestrians	56
CBR traffic packet size	4,096 bits
CBR traffic packet inter-arrival time	4 slots

A. Simulation Assumptions

The considered scenario has one bus that serves 6 passengers through its IAB node, which is traveling with a constant speed of 50 km/h on a trajectory that passes in front of 3 building blocks modeled using a simplified Madrid Grid [12], [13] (see Fig. 2). One IAB donor is placed at the end of the opposing side of each block, from where the IAB node passes. 40 pedestrians moving with a speed of 3 km/h are connected to the central IAB donor, while the other IAB donors serve only 5 pedestrians, each. We consider 22 resource blocks (RBs), that are shared by all the network nodes. Also, a constant bit rate (CBR) traffic model is assumed, generating packets with size 4.096 bits each 1 ms. The values of the simulation parameters are presented in Tables I and II.

In order to avoid self-interference, IAB-DU and IAB-MT operate in half duplex (HD), meaning that they cannot transmit while the other is receiving, i.e., they operate together in the same direction, either both transmitting or receiving.

B. Simulation Results

This section presents: 1) the duration of the mIAB node's connection to each IAB donor; 2) the time evolution of buffer size of access and backhaul links; and 3) the uplink (UL) and downlink (DL) throughput for pedestrians and passengers.

B.1 mIAB node connection time

In Fig. 3, we present the total time the mIAB node (bus) is connected with each IAB donor, with and without usage of

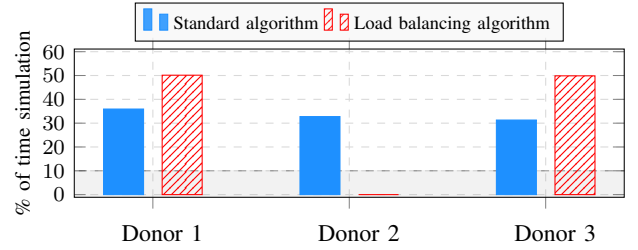


Fig. 3. Total time the mIAB remains connected with donors 1, 2 and 3 with the standard and load balancing algorithms.

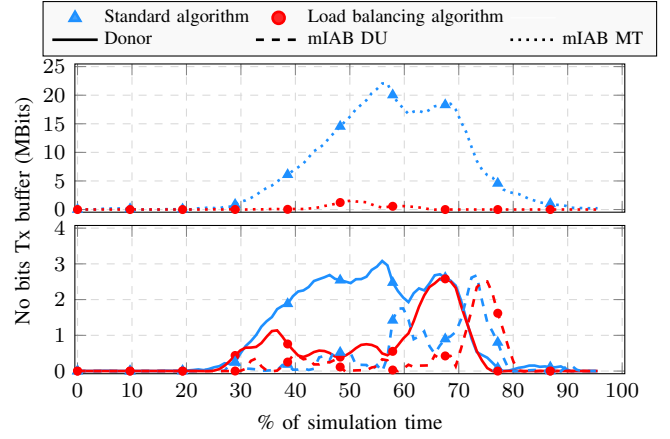


Fig. 4. Number of buffered bits in the mIAB MT to be transmitted in the UL backhaul (dotted), IAB donors to mIAB links (solid) and in the mIAB to passengers links (dashed).

the proposed the load balancing TA. We can see that using the standard TA algorithm [9], the mIAB node remains connected to each IAB donor approximately 33% of the simulation time, as expected considering the IAB node constant speed and the grid symmetry. When Algorithm 1 is used, there is no connection between the mIAB node and the overloaded central block IAB donor. This means the algorithm effectively accounts for the overload in the TA process, improving QoS for passengers by ensuring more resources are available in its serving IAB donor.

B.2 Transmission Buffer Load

In Fig. 4, we present the time evolution of the amount of buffered bits in different nodes in the system: bits in mIAB MT (dotted curves), IAB donors (solid curves) and mIAB DU (dashed curves). The curves for standard solution and proposed solutions are represented by blue and red curves, respectively.

Focusing firstly in the UL backhaul, i.e., mIAB MT, we can see that our proposed solution results in a significantly lower accumulation of buffered bits, especially halfway through the simulation, when the bus is closer to the central IAB donor, as expected, since the connection between the mIAB node and the overloaded IAB donor is prevented. When the DL access and backhaul at IAB donors are regarded, we can also observe a lower bits accumulation for our proposed solution. However, the decrease in buffer accumulation with our proposal compared to the standard solution is not at the same level as in UL backhaul mIAB MT. The reason is that interference becomes more critical in the DL when the bus

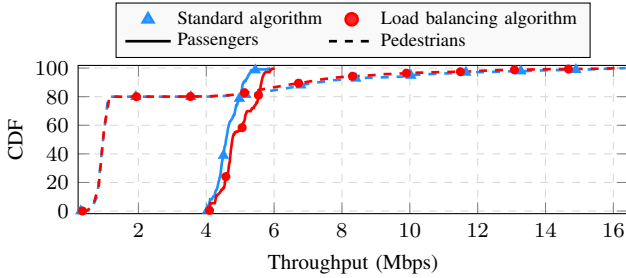


Fig. 5. UL throughput CDF for the two studied topology adaptation algorithms.

passes in front of the second block, since the closest IAB donor (the one at the central block) providing the highest RSRP becomes a major source of interference to the backhaul in DL. This higher interference leads to lower throughput that causes the buffer clogging.

Fig. 4 also shows the number of bits at the DL access of mIAB DU. Interestingly, the load accumulation, in this case, takes place mainly during the last part of the simulation. This happens because after the bus passes through the second block, it finally connects to the rightmost IAB donor which has more resources to serve it in the DL backhaul. Then, the rightmost IAB donor starts to send the packets that were previously clogged in the overloaded IAB donor (in the central block), which in turn overloads temporarily the mIAB node buffer. We can also see that when using Algorithm 1, the buffer size accumulation is lower at first but becomes higher during 70% to 80% of the simulation time.

B.3 UL Throughput

In Fig. 5, we present the cumulative distribution function (CDF) of passengers (solid curves) and pedestrian (dashed curves) UL throughput for the proposed (red curves) and standard solutions (blue curves). For passengers, the proposed solution shows throughput gains over the standard solution. At the 90th percentile, the throughput for the proposed and standard solutions are of 5.63 Mbps and 5.11 Mbps, respectively, which leads to a performance gain of approximately 10%. For the 10th percentile, the performance gain is more modest (2.3%). The gains were more prominent in the higher percentiles due to, e.g., the random nature of the pedestrian positioning, which may cause them to become closer to the mIAB node causing more interference in some iterations of the simulation.

For pedestrians, note that our proposal leads to a slight throughput degradation in the highest percentiles. The reason for this is that the proposed solution connects the mIAB node with the less overloaded IAB donors for a longer time. Thus, the pedestrians from these IAB donors, which have the highest throughputs (highest percentiles in the plot), have to share radio resources with the mIAB node leading to a throughput degradation. For the same reason, we would expect a throughput improvement for pedestrians at the central block (lower percentiles in the plot) with the proposed solution compared to the standard one. However, as there are too many

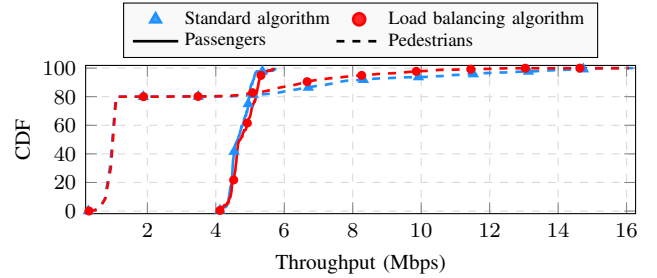


Fig. 6. DL throughput CDF for the two studied topology adaptation algorithms.

pedestrians to share the system resources in this block, the throughput improvement is not noticeable.

B.4 DL throughput

In Fig. 6, we present the CDF of passengers (solid curves) and pedestrian (dashed curves) DL throughput for the proposed (red curves) and standard solutions (blue curves). We can see that there was a general improvement in QoS for passengers, but not as expressive as for the UL scenario. While in the 90th percentile the proposed solution achieves a performance gain of 1.1%, no performance gain can be seen in the 10th percentile. These lower gains in DL throughput for passengers can be explained by the increased backhaul interference the mIAB node experiences, particularly when it passes in front of the overloaded IAB donor (as previously explained).

For pedestrians, the performance of the proposed and standard solutions are very similar, except at the higher percentiles where our solution presents a performance loss of 13% at the 90th percentile. The reason is the same as stated for the UL performance in Fig. 5: with the proposed solution, the less loaded IAB donors have to share their resources for a longer time with the mIAB node which leads to performance degradation for the pedestrians with higher throughputs. Despite this performance loss, the throughput of 6.67 Mbps achieved at the 90th percentile for the proposed solution is still considered a good QoS for mobile applications.

V. CONCLUSIONS

This work investigated and compared a standard RSRP-only based TA algorithm with a proposed solution that additionally takes into account the load in the network nodes. Based on our analyses, the proposed solution significantly reduced the amount of buffered bits, outperforming the standard solution in terms of throughput for passengers. Our proposed solution negatively affected the performance of pedestrian UEs, but mostly the ones with over provision of QoS. Therefore, the proposed solution effectively enhances the overall QoS for passengers without significantly compromising the performance of pedestrians.

REFERENCES

- [1] R. Flamini, D. De Donno, J. Gambini, *et al.*, "Towards a heterogeneous smart electromagnetic environment for millimeter-wave communications: An industrial viewpoint," *IEEE Trans. Antennas Propag.*, vol. 70, no. 10, pp. 8898–8910, Feb. 2022. DOI: 10.1109/TAP.2022.3151978.

- [2] R. A. Ayoubi, M. Mizmizi, D. Tagliiferri, D. D. Donno, and U. Spagnolini. "Network-controlled repeaters vs. reconfigurable intelligent surfaces for 6G mmW coverage extension." arXiv: 2211.08033. (Nov. 2022).
- [3] M. Polese, M. Giordani, T. Zugno, *et al.*, "Integrated access and backhaul in 5G mmWave networks: Potential and challenges," *IEEE Commun. Mag.*, vol. 58, no. 3, pp. 62–68, Mar. 2020. DOI: 10.1109/MCOM.001.1900346.
- [4] C. Madapatha, B. Makki, C. Fang, *et al.*, "On integrated access and backhaul networks: Current status and potentials," *IEEE Open J. Commu. Soc.*, vol. 1, pp. 1374–1389, Sep. 2020. DOI: 10.1109/OJCOMS.2020.3022529.
- [5] V. F. Monteiro, F. R. M. Lima, D. C. Moreira, *et al.*, "TDD frame design for interference handling in mobile IAB networks," in *Proc. of the IEEE Global Telecommun. Conf. (GLOBECOM)*, Dec. 2022, pp. 5153–5158. DOI: 10.1109/GLOBECOM48099.2022.10001454.
- [6] O. Teyeb, A. Muhammad, G. Mildh, E. Dahlman, F. Barac, and B. Makki, "Integrated access backhauled networks," in *Proc. of the IEEE Vehic. Tech. Conf. (VTC)*, Honolulu, HI, USA, Nov. 2019, pp. 1–5. DOI: 10.1109/VTCFall.2019.8891507.
- [7] 3GPP, "Study on vehicle-mounted relays; stage 1 (release 18)," 3rd Generation Partnership Project (3GPP), TR 22.839, Sep. 2021, v.18.0.0. [Online]. Available: <http://www.3gpp.org/ftp/Specs/html-info/22839.htm> (visited on 10/20/2021).
- [8] 3GPP, "NR; study on integrated access and backhaul (release 16)," 3rd Generation Partnership Project (3GPP), TR 38.874, Dec. 2018, v.16.0.0. [Online]. Available: <http://www.3gpp.org/ftp/Specs/html-info/38874.htm> (visited on 04/13/2021).
- [9] V. F. Monteiro, F. R. M. Lima, D. C. Moreira, *et al.*, "Paving the way towards mobile IAB: Problems, solutions and challenges," *IEEE Open J. Commu. Soc.*, vol. 3, pp. 2347–2379, Nov. 2022. DOI: 10.1109/OJCOMS.2022.3224576.
- [10] M. Choi and H. Chung, "Relay node load balancing method in mobile communication environment," in *Proc. of the IEEE Internat. Conf. on Information and Communication Technology Convergence*, 2021, pp. 1–3. DOI: 10.1109/ICTC52510.2021.9620816.
- [11] 3GPP, "NR; NR and NG-RAN Overall description; Stage 2," 3rd Generation Partnership Project (3GPP), TS 38.300, Jul. 2020, v.16.2.0. [Online]. Available: <http://www.3gpp.org/ftp/Specs/html-info/38300.htm> (visited on 04/13/2023).
- [12] P. Agyapong *et al.*, "Simulation guidelines," METIS, Deliverable 6.1, Oct. 2013. [Online]. Available: https://metis2020.com/wp-content/uploads/deliverables/METIS_D6.1_v1.pdf (visited on 09/20/2021).
- [13] Y. Sui, I. Guvenc, and T. Svensson, "Interference management for moving networks in ultra-dense urban scenarios," *Journal of Wireless Commun. and Netw.*, vol. 111, pp. 1–32, Apr. 2015. DOI: 10.1186/s13638-015-0326-1.
- [14] 3GPP, "Study on channel model for frequencies from 0.5 to 100 GHz," 3rd Generation Partnership Project (3GPP), TR 38.901, Sep. 2017, v.14.2.0. [Online]. Available: <http://www.3gpp.org/DynaReport/38901.htm> (visited on 09/26/2017).
- [15] 3GPP, "Study on evaluation methodology of new vehicle-to-everything (V2X) use cases for LTE and NR," 3rd Generation Partnership Project (3GPP), TS 37.885, Dec. 2018, v.15.2.0. [Online]. Available: <http://www.3gpp.org/ftp/Specs/html-info/37885.htm> (visited on 04/17/2019).